González-Herráez, M., Fernández-Ruiz, M.R., Magalhäes, R., Costa, L., Martins, H.F., García-Ruiz, A., Martín-López, S., Williams, E., Zhan, Z. & Vantilho, R. 2019, "Photonic Seismology", in International Photonics and OptoElectronics Meeting 2019 (OFDA, OEDI, ISST, PE, LST, TSA), The Optical Society (OSA, 2019), paper OFTu3A.2.

Available at https://doi.org/10.1364/OFDA.2019.OFTu3A.23A.2

Photonic Seismology

Miguel Gonzalez-Herraez[*,1], **Maria R. Fernandez-Ruiz**[1], **Regina Magalhaes**[1], **Luis Costa**[1], **Hugo F. Martins**[2], **Andrés Garcia-Ruiz**[1], **Sonia Martin-Lopez**[1], **Ethan Williams**[3] , **Zhongwen Zhan**[3] **and Roel Vantilho**[4]
[1]*Dpto. de Electrónica, University of Alcalá, 28805, Alcalá de Henares (Madrid), Spain*
[2]*Instituto de Óptica, CSIC. C/Serrano 121. 28006, Madrid, Spain*
[3]*Seismological Laboratory, California Institute of Technology, Pasadena, CA 91125-2100, USA*
[4]*Marlinks, Sint-Maartenstraat 5, 3000 Leuven, Belgium*
*miguel.gonzalezh@uah.es

Abstract: One of the greatest outstanding challenges in seismology is the sparsity of instrumentation across the Earth, particularly in the oceans. In this work we show that optical fiber-based distributed acoustic sensors (DAS) can represent a low-cost solution (basically inexistent so far) for monitoring seismicity in remote areas of the ocean. This solution can retrofit existing telecommunication optical fiber cables lying in the ocean and transform them (with no basic change in the cable itself) into powerful seismic sensing arrays. With a single optoelectronic unit in the end of the cable (onshore), a full span of 50-100 km can be monitored, with thousands of measuring points interrogated.

OCIS codes: (060.2370) Fiber optics sensors; (290.5870) Scattering, Rayleigh; (280.0280) Remote sensing and sensors; (120.4825) Optical time domain reflectometry; (280.7250) Velocimetry.

1. Introduction

Seismic tomography is a powerful tool for imaging the Earth structure by using earthquakes and other terrestrial wave sources. Currently, tomographic methods in seismology rely on the existing network of conventional seismometers spread around the word. Unluckily, this network is quite inhomogeneous, mainly distributed onshore over North America, Europe and in certain regions of known strong seismic activity. Consequently, the sole use of this network results in the acquisition of biased and low spatially-sampled information. The deployment and maintenance of a more homogeneous cluster of conventional seismometers around the Earth results practically and economically inviable, as many of these seismometers would have to be installed in the ocean. Interestingly, the availability of more than 1 million kilometers of optical cable in the world (mainland and across the oceans), arises the interesting alternative to re-use of the telecommunication fiber network as a distributed sensor for seismic monitoring. Distributed acoustic sensors (DAS) have been recently proposed for distributed sensing of seismic activity around the Earth[1,2]. This technique allows to re-purpose the deployed telecommunication fiber optic network for detecting and monitoring seismic activity at different locations of an optical fiber cable, with a spatial resolution in the order of meters.

Recently, a novel DAS based on phase-sensitive (φ)OTDR has been introduced, known as chirped-pulse φOTDR (CP-φOTDR)[3]. This system has proven capable of quantifying the magnitude of ongoing perturbations over the fiber with record sensitivities[4] for a distributed sensor, improved performance[5] and simpler setup than traditional configurations. With traditional configurations, we mean other schemes capable of quantifying the perturbation, such as those based on coherent detection (requiring polarization diversity and phase diversity)[6] or using laser frequency sweeping strategies (requiring a highly coherent tunable laser source and heavy post-processing)[7]. Using CP-φOTDR, we have detected an M8.2 earthquake occurred in Fiji Island last August, 2018 from two different locations with very different environmental conditions and placed >9,000 km away from the earthquake epicenter. On the one hand, we have measured the earthquake from a densely populated metropolitan area in Pasadena, CA, USA. On the other hand, the earthquake was detected from a shallow submarine fiber in the city of Zeebrugge, Belgium. Such a different, noisy locations ensure a thorough analysis of the possibilities of the optical fiber to monitor teleseism activity. The results shown represent a firm step forward in the use of the telecommunication fiber optical network as distributed seismometers.

2. Sensor deployment

The distributed sensing method known as CP-φOTDR was introduced several years ago[3] as an alternative technique to quantify the detected perturbation with much simpler optical arrangement than existing methods to date[7,8]. Similar to classical φOTDR, the method launches a train of optical pulses over a fiber and compares successive Rayleigh backscattered traces in order to detect a perturbation. Whenever a strain or temperature perturbation affect the fiber, the central frequency of the propagating light is slightly shifted by an amount proportional to the perturbation. In CP-φOTDR, a sufficiently high linear chirp is induced into the input pulse. Then, a frequency-to-time mapping occurs in the fiber and the directly-detected temporal trace suffers a time shift locally over the perturbation position. This modification entails important advantages, such as the simplicity in the employed setup, the robustness against laser phase noise and the record sensibilities achievable[4,5]. The employed optical setup of the fiber interrogator unit is represented in Fig. 1(a), where we can see that a distributed amplification stage (i.e, Raman amplification) has been added to the system to increase its operating range[8].

Two interrogation units identical to the one described in the previous Section are placed in two different locations and connected to already-deployed fiber optic cables. In the city of Pasadena, we use a 25 km fiber that is part of the local telecommunication network. Its geometrical distribution is plotted in Fig. 1(b), together with a map of the real fiber distribution. In the inset of Fig. 1(b), we can observe that the fiber includes several loops that contribute to increase the length with respect to the geometrical distance occupied by the fiber. In this location, the main source of noise comes from traffic and other human activity. In the city of Zeebrugge, we use a 40 km fiber deployed perpendicular to the shore, reaching almost 33 m of depth (see Fig. 1(c)). The fiber was deployed there to monitor a power cable from an offshore wind farm. Such a shallow fiber is highly exposed to superficial noise, such as ocean waves or ship-induced noise.

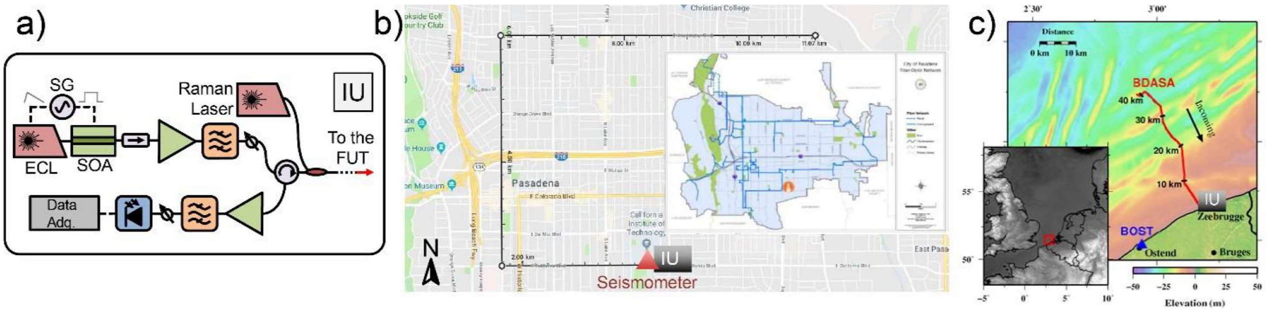

Figure 1. (a) Setup of CP-φOTDR employed for the experimental tests. ECL: External cavity laser, SG: Signal generator, SOA: semiconductor optical amplifier, FUT: fiber under test, IU: Interrogator unit. (b) Geometrical distribution of the fiber in Pasadena, including the location of the reference seismometer, the interrogator unit, and an inset with the real distribution of the fiber over the city. (c) Map of the fiber distribution in the cost of Zeebrugge, including the location of the seismometer (BOST), the interrogator unit, and an inset with the location of the fiber over the north shore of Europe.

3. Results

The traces acquired by the interrogator unit from each of the launched pulses can be plotted forming a waterfall, in such a way they form a 2D image in which the abscissa represents measurement time and the ordinate represents fiber length. As the environment in the measurement locations is especially noisy, the raw acquired data must be processed to implement a denoising process. We have selected to use a simple 2D rectangular-like band-pass filter to isolate the spectral bands of the earthquake signal from the rest of the detected vibrations. In particular, by having previous knowledge of the typical spectral content of seismic activity, we have selected the transition bands of the filter at 0.02 Hz and 1 Hz for the temporal frequency axis and at 0 and $4\cdot10^{-4}$ m^{-1} for the spatial frequency axis. Once the filter is applied, most of the noise in the measurements is eliminated, and the remaining signal energy can be associated to earthquake information. The resulting data is analyzed by comparing the filtered signal with the trace acquired by nearby seismometers (see Fig. 1(a) and (b)). For this purpose, we stack the traces of the last 5 km of fiber in each location. In Pasadena, the reason is that the last 5 km corresponds to fiber directed from West to East location, which coincides with the direction of propagation of the earthquake. Hence, the CP-φOTDR trace is compared with the seismometer trace in the West-East direction. In Zeebrugge, however, the main reason of taking the last 5 km of fiber is that they correspond with the deepest fiber, and therefore the noise of the associated traces is lower. In this case, the traces from the seismometers in the West-East and North-South directions are rotated to the fiber azimuth for the comparison. In order to compare the arriving frequency components along the time, we compare the spectrograms of the CP-φOTDR stacked trace and the seismometers. The results are discussed in the following sub-sections.

Figure 2 presents the comparison between the spectrograms of the stacked CP-φOTDR trace (Fig. 2(a)) and the seismometer trace (Fig. 2(b)). We can observe that the earthquake starts around 1000 s. The difference in the starting time in both instruments is due to a delay in the beginning or the recording. We can observe that the time-frequency dynamic is similar in both measurements. In particular, right at the beginning of the earthquake, higher frequencies arrive, up to 1 Hz. Those correspond to primary waves. After that, the maximum frequency components of the signal are reducing along the time, finding some peaks associated to crust-reflected primary waves and secondary waves, respectively. The difference in the magnitude of the obtained data is due to the fact that CP-φOTDR measures fiber strain perturbations while the spectrometers measures particle velocity. Even if these magnitudes are not directly comparable, they are almost proportional, permitting a rough comparison.

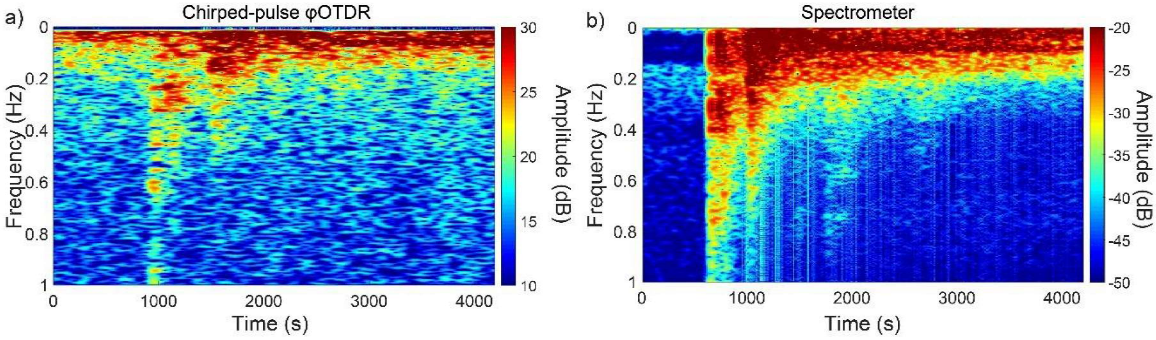

Figure 2. Results from Pasadena: spectrograms of the stacked CP-φOTDR trace (a) and the seismometer trace (b).

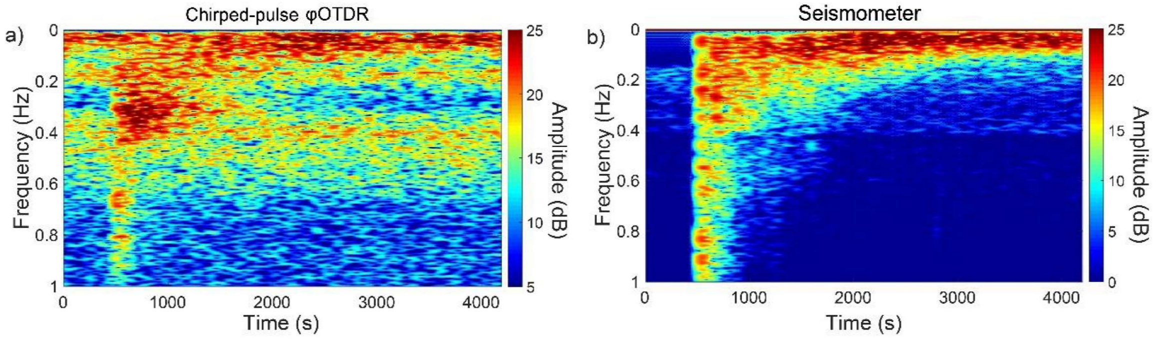

Figure 3. Results from Zeebrugge: spectrograms of the stacked CP-φOTDR trace (a) and the seismometer trace (b).

Figure 3(a) shows the spectrogram of the stacked traces acquired via CP-φOTDR, and Fig. 3(b) shows the seismometer trace. We can observe similar behavior than in the case of Pasadena. However, constant frequency components around 0.2 Hz and 0.4 Hz appears in the CP-φOTDR trace that are not related to the earthquake (those components do not appear in Fig. 3(b)). The component at 0.2 Hz corresponds to ocean waves and the one at 0.4 Hz is related to microseisms associated to the former ones. A deep analysis of these kind of waves is out of the scope of this communication. Still, it is possible to realize the strong potential of DAS for monitoring submarine seismic activity.

4. Conclusions

In this communication, we have demonstrated the viability of using the already-deployed telecommunication optical fiber network for the monitoring of seismic activity around the word. Hence, we have detected an M8.2 earthquake occurred in Fiji Island from two different locations with very distinctive environmental features. In spite of the great differences in terms of noise, we have performed a similar analysis in both cases, namely, the application of a linear 2D band-pass filter to a waterfall of CP-φOTDR traces. The resulted data is compared with data acquired by nearby seismometers, verifying the similarities in the obtained results. The presented results may give place to important developments in the field of seismic topography.

This work was supported by European Commission (EC) (H2020) through the FINESSE project, (MSCA-ITN-ETN-722509); Ministerio de Economía y Competitividad (MINECO, project TEC2015-71127-C2-2-R); Ministerio de Ciencia, Innovación y Universidades (MICINN) (IJCI-2017-33856, RTI2018-097957-B-C31); Comunidad de Madrid (CM) and FEDER program (SINFOTON2-CM: P2018/NMT-4326) and University of Alcalá (FPI grant).

4. References

[1] Jousset, P., et al.., Nat. Commun., 9(2509), 1–11 (2018).
[2] Ajo-Franklin, J. B., et al., Sci. Rep., 9(1328), 1-14 (2018).
[3] Pastor-Graells, J. et al., Opt. Express, 24(12), 13121-13133 (2016).
[4] Costa, L. et al., J. Lightwave. Technol., early access.
[5] Fernández-Ruiz, M. R. et al. J. Lightwave. Technol., 36(23), 5690-5696 (2018).
[6] Pan, Z et al., Opt. Sensors Biophotonics, 8311(8), 83110S (2011).
[7] Koyamada, Y., et al. J. Light. Technol., 27(9), 1142–1146 (2009).
[8] Pastor-Graells, J et al. J. Lightw. Technol., 35(21), 4677–4683 (2017).